

UHF Resonator with Linear Tuning*

B. H. WADIA† AND R. L. SARDA†

Summary—A novel method of tuning a transmission-line type resonator is described. The first-order theory of such a resonator is derived and presented in the form of design curves which indicate an extremely good tuning linearity. Experiments with a resonator designed on this principle agree with theory.

I. INTRODUCTION

A tunable resonant device, in which frequency varies linearly with mechanical motion, promises a large number of advantages in applications such as wavemeters, ganged resonators, and mechanically swept oscillators where such a characteristic could permit vernier frequency dials, one-point calibration, and easier alignment and adjustment. Resonant circuits which are in general use (LC circuits, resonant lines, re-entrant cavities) depart greatly from linearity when used over a large frequency range. Attempts are often made to improve linearity by special measures and auxiliary devices such as cams, link motions, specially shaped tuning rods and plates; among the more sophisticated devices of this type, we may mention the developments of Ginzton and Salisbury,¹ and Brot and Soulard.² However, these methods are not linear "in principle" but are made so by special design. A resonant system which can indicate linearity or near linearity in its basic conception is likely to be even more valuable.

This paper describes a simple method of tuning which exhibits good linearity over a wide frequency range. In essence, it involves two quarter-wave resonant transmission line sections which are coupled together at their open ends by a series capacitor. By a common mechanical motion, the length of one section is increased while that of the other is reduced by the same amount in such a way that the combined length remains the same. This causes one section of line to tune up its frequency curve while the other tunes down and the nonlinearities of the two sections effectively cancel each other. By a proper choice of the characteristic impedances of the two sections, one can vary the tuning range, the rate of tuning, and the region of approximate linearity. This principle is quite neatly applied to two quarter-wave coaxial lines placed "back-to-back" so as to form a doubly re-entrant cavity as shown in Fig. 1(a); tuning is accomplished by the movement of the capacitive gap relative to the outer conductor. The theory and the design curves for this type of tuning are derived and show that good line-

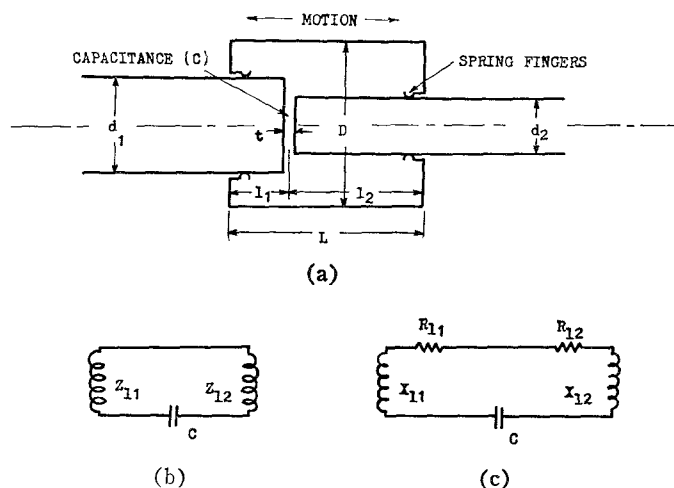


Fig. 1—(a) Schematic diagram of the resonant system. (b) Idealized and lossless equivalent circuit. (c) Ideal equivalent circuit with losses.

arity can be obtained over as large a tuning range as 1.5:1. Experimental evidence is given in support of the theory. The study also includes a consideration of the higher order modes and the *Q* of the structure.

In connection with previous work, we may mention an article by Barrow and Mieher³ which gives extensive experimental data on re-entrant cavities. The article deals with various modes which interplay in a re-entrant cavity as it passes from a perfect cylinder to a perfect coaxial line. In the process, the authors give brief data on the resonant frequencies of the cavity with various gap positions. It is interesting to note its similarity with the data presented in our work. However, Barrow and Mieher do not proceed to analyse the system nor to consider it as a method of linear tuning as is done in the present paper. The article came to the attention of the authors after the principle of back-to-back tuning had been established.

II. PRINCIPLE OF BACK-TO-BACK TUNING

Consider two coaxial line sections each shorted at one end with their open ends brought together. If the diameters of their outer conductors are equal and if a narrow capacitive gap is left at the junction between their center conductors, a doubly re-entrant resonant cavity results. Fig. 1(a) shows such a structure and its major dimensions. In general, the diameters (d_1 and d_2) of the two portions of the center conductor on either side of the capacitive gap may be different; they are,

* Manuscript received by the PGMTT, June 12, 1959.

† Central Electronics Engrg. Res. Inst., Pilani, Rajasthan, India.

¹ E. L. Ginzton and F. L. Salisbury, "Ultra-high-frequency wavemeter," U. S. Patent No. 2,503,256; April, 1950.

² C. Brot and A. Soulard, "Cavity with linear tuning for meter and decimeter wavelengths," *Compt. Rend. Acad. Sci. (Paris)*, vol. 243, pp. 1848-1850; December, 1956.

³ W. L. Barrow and W. W. Mieher, "Natural oscillations of electrical cavity resonators," *PROC. IRE*, vol. 28, pp. 184-191; April, 1940.

however, mechanically joined together to keep the gap distance constant. Tuning of the cavity consists in making the outer shell capable of axial motion relative to the center conductor assembly so that the capacitive gap changes position and the lengths of the two coaxial lines on either side of the capacitive gap are altered by the same amount—one increases and the other decreases in length. If l_1 and l_2 are the lengths of the two sections and Z_{01} and Z_{02} are their characteristic impedances, the ideal and lossless equivalent circuit of the resonator will be as shown in Fig. 1(b). The impedances of the two lines in question seen at the capacitive gap will be

$$Z_{l_1} = jZ_{01} \tan \frac{2\pi l_1}{\lambda},$$

$$Z_{l_2} = jZ_{02} \tan \frac{2\pi l_2}{\lambda};$$

both are normally inductive.

A. The Resonance Equation

For resonance

$$\frac{1}{2\pi f C} = Z_{01} \tan \frac{2\pi l_1}{\lambda} + Z_{02} \tan \frac{2\pi l_2}{\lambda}.$$

By appropriate re-arrangement

$$\frac{1}{\left(\frac{2\pi f L}{v_0}\right) \left(\frac{C Z_{01} v_0}{L}\right)} = \tan \left[\left(\frac{2\pi f L}{v_0} \right) \left(\frac{l_1}{L} \right) \right] + \left(\frac{Z_{02}}{Z_{01}} \right) \tan \left[\left(\frac{2\pi f L}{v_0} \right) \left(1 - \frac{l_1}{L} \right) \right],$$

where v_0 = velocity of light.

It is noted that the bracketed quantities are dimensionless and constitute normalized variables. A simpler form of the equation results as

$$\frac{1}{f_n C_n} = \tan f_n l_{1n} + Z_n \tan f_n (1 - l_{1n}) \quad (1)$$

where

$$f_n = \text{normalized resonant frequency} = \frac{2\pi f L}{v_0}, \quad (2)$$

$$l_{1n} = \text{normalized length} = \frac{l_1}{L}, \quad (3)$$

$$C_n = \text{normalized impedance} = \frac{C Z_{01} v_0}{L}, \quad (4)$$

$$Z_n = \text{normalized impedance} = \frac{Z_{02}}{Z_{01}}. \quad (5)$$

In order to examine the tuning characteristics, the above equation must be solved to yield f_n as a function of l_{1n} for representative values of the design parameters Z_n and C_n . From the nature of the above equation it would at first appear that the relation between f_n and

l_{1n} could hardly be linear and indeed in the rigorous sense it is not so; attempts to convert (1) to a linear form by some appropriate approximation did not yield neat results. However, solution and plotting of (1) shows that a significant portion of the curve differs only slightly from the linear, and this is borne out by subsequent experimentation. It must be admitted that, in spite of the nonlinear appearance of (1), faith in the ultimate linearity of tuning was maintained by a certain amount of intuitive reasoning based on the fact that the two component lines of the resonator are operating back-to-back; while one is increasing in length, the other is being reduced—thus giving a chance for the nonlinearities on either side of the gap to neutralize each other.

B. Solution of the Resonance Equation

By treating Z_n and C_n as parameters, (1) reduces to an implicit transcendental relation between f_n and l_{1n} for each set of values of Z_n and C_n and can be solved by well-known graphical methods. For each value of l_{1n} from 0 to 1, the two sides of the equation are separately plotted with f_n as abscissa; the intersection of the two curves gives the solution of f_n for each l_{1n} . Fig. 2 pertains

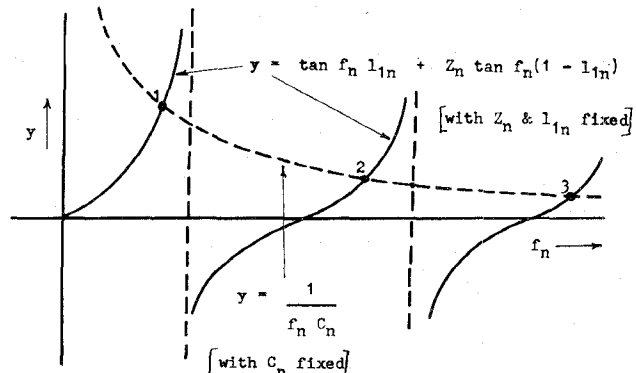
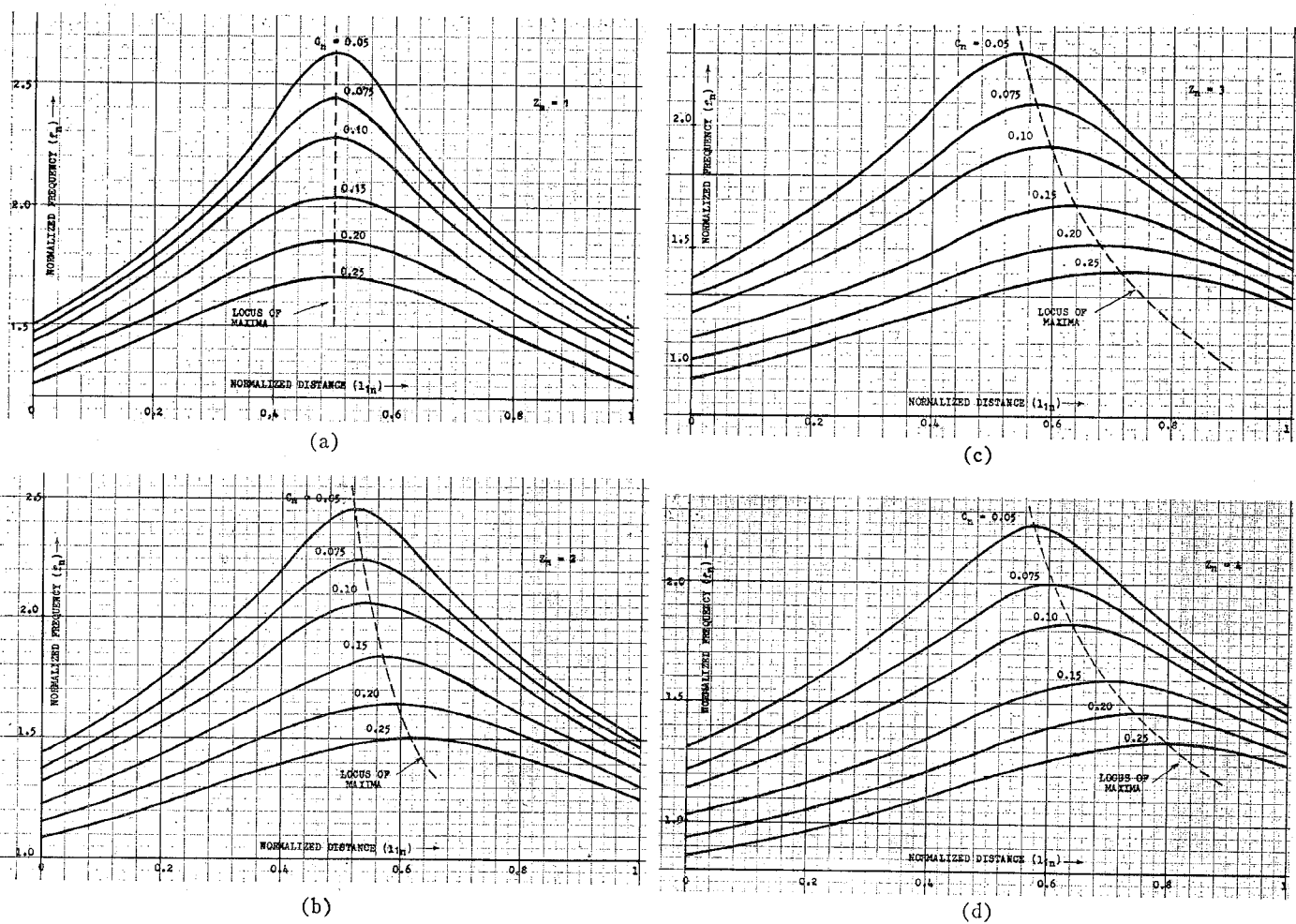


Fig. 2—Method of solution of the resonance equation.

to this process of graphical solution. It must be noted that the terms on the right hand side of the equation are periodic and that there will be a large number of possible solutions according to the branch on which the intersection occurs. We shall discuss this point again later, but for the moment we limit ourselves to the solution on the first branch of the curve, thus considering only the case of "quarterwave" operation for each of the two component lines. This is the lowest or dominant mode and is of major practical importance.

The solutions obtained for this fundamental mode are given in Fig. 3(a), (b), (c), and (d) in the form of a series of universal design curves. These curves and the normalized variables defined in (2), (3), (4) and (5) give us the tools for designing these types of resonators in the desired frequency range. The loci of the maxima are also obtained by equating the derivative to zero and solving the resulting equation.

Fig. 3—Universal design curves for various values of Z_n and C_n .

An examination of these curves shows the following properties:

- 1) Good linearity is obtained except near the maximum of the curve.
- 2) For values of Z_n other than unity, better linearity and more gradual tuning can be obtained over a greater range on one side of the curve than on the other.
- 3) The tunable range is reduced while linearity improves as value of C_n increases.
- 4) From symmetry considerations, it should be clear that for Z_n less than unity, the curves are lateral inversions of the corresponding cases for their reciprocals.
- 5) For $l_{1n}=0$ or 1 the cavity resembles a singly re-entrant cavity of length L and characteristic impedance Z_{02} or Z_{01} respectively.

C. Higher Order Modes

We have thus far restricted ourselves to the discussion of the simplest mode in the cavity, *i.e.*, the transmission line mode with nearly quarterwave variation in each coaxial section. It would be worthwhile to study the possibility of other modes to see whether they behave linearly and to assure that there is no likelihood of

interference between the useful mode and the higher orders.

That higher order longitudinal modes are possible can easily be seen from the periodic nature of the tangent functions and from Fig. 2, where several intersections are indicated. A physical picture can also be obtained by noting that the resonance condition is determined by the impedances looking into both lines at the plane of the capacitive gap; the requisite impedances on either side may be obtained by modes which are not necessarily of the fundamental type. The number of possibilities for satisfying the resonance condition is therefore infinite for each position of the capacitive gap.

For a proper understanding of such higher modes, a solution for some typical values of parameters was obtained for the mode which appears next after the dominant, *i.e.*, as given by the second intersection (shown in Fig. 2). Fig. 4 shows a comparison of the normal tuning curve with the tuning curve for this next solution when $Z_n=3$ and $C_n=0.05$. It is noted that the new curve is far from regular; also that, fortunately, considerable frequency separation occurs, and there is no harmonic relation between the modes. We are therefore fairly safe in assuming good mode-separation properties.

Higher order modes of the circumferential type are

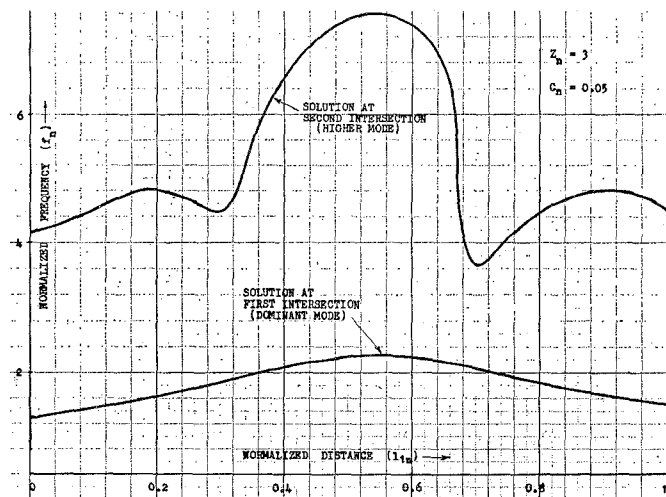


Fig. 4—Comparison of the next higher mode with the dominant for $Z_n = 3$, and $C_n = 0.05$.

also possible as in all cylindrically symmetric structures. However, if care is taken to keep the circumference of the cavity sufficiently less than one wavelength in the operating range, the cavity can be essentially free from circumferential mode interference.

Two simple checks can be made to assure that any given design is operating in the required fundamental mode:

$$\pi D \ll \lambda \quad \text{for circumferential modes}$$

$$2L < \lambda \quad \text{for longitudinal modes}$$

at the highest operating frequency.

III. CALCULATION OF Q

If we take into account the small losses occurring in the cylindrical conducting walls, the equation of input impedance of the left side line can be rewritten as

$$Z_{l_1} = R_{l_1} + jX_{l_1} = Z_{01} \tanh \gamma_1 l_1$$

where

$$\gamma_1 = \alpha_1 + j\beta_1,$$

α_1 = loss factor in nepers per meter (small),

β_1 = phase constant in radians per meter

provided we neglect the losses at the shorting end and at the capacitive gap.

By standard algebraic methods, the real and the imaginary parts of the above equation can be separated to give

$$Q_0 = \frac{Z_{01} \left(\frac{D}{d_1} \right) L^{1/2}}{2.774 \times 10^{-4} f_n^{3/2} C_n \left[\left(\frac{D}{d_1} + 1 \right) l_{1n} \sec^2 f_n l_{1n} + \left(\frac{D}{d_2} + 1 \right) (1 - l_{1n}) \sec^2 f_n (1 - l_{1n}) \right]}$$

$$R_{l_1} = Z_{01} \alpha_1 l_1 \sec^2 \beta_1 l_1$$

$$X_{l_1} = Z_{01} \tan \beta_1 l_1.$$

We assume that α_1 is quite small so that terms with $\alpha_1^2 l_1^2$ are neglected and $\tan \alpha_1 l_1 \approx \alpha_1 l_1$. This assumption is justified for cavities with inner surfaces of high conductivity materials.

The value of α_1 is given by the usual skin effect formula⁴; for a silver plated cavity

$$\alpha_1 = \frac{6.68 \times 10^{-10} \sqrt{f} \left(\frac{D}{d_1} + 1 \right)}{D \log_e \frac{D}{d_1}}.$$

But since

$$Z_{01} = 60 \log_e \frac{D}{d_1} \quad \text{and} \quad f_n = \frac{2\pi f L}{v_0},$$

hence

$$\alpha_1 = 2.774 \times 10^{-4} \sqrt{\frac{f_n}{L}} \cdot \frac{\left(\frac{D}{d_1} + 1 \right)}{Z_{01} D}. \quad (6)$$

The resistive and reactive components of Z_{l_1} become

$$R_{l_1} = 2.774 \times 10^{-4} \sqrt{\frac{f_n}{L}} \cdot \frac{\left(\frac{D}{d_1} + 1 \right)}{\frac{D}{L}} l_{1n} \sec^2 f_n l_{1n}$$

$$X_{l_1} = Z_{01} \tan f_n l_{1n}$$

and similar expressions hold for the right-side coaxial line.

The equivalent circuit of Fig. 1(b) can be modified to include the resistive components as shown in Fig. 1(c). An expression for the unloaded Q is then simply given by

$$Q_0 = \frac{X_{l_1} + X_{l_2}}{R_{l_1} + R_{l_2}}.$$

But we note that

$$X_{l_1} + X_{l_2} = Z_{01} \tan f_n l_{1n} + Z_{02} \tan f_n (1 - l_{1n}) = \frac{Z_{01}}{f_n C_n}.$$

Hence

$$Z_{01} \left(\frac{D}{d_1} \right) L^{1/2}$$

⁴ W. Jackson, "High Frequency Transmission Lines," Methuen and Co. Ltd., London, Eng., p. 50; 1951.

IV. EXPERIMENTAL RESULTS

A. Cavity Design

In most cases, cavity design begins with a knowledge of the desired tuning range around a given center frequency. From the normalized curves in Fig. 3, one curve with the appropriate linear tuning range and slope is chosen; this determines the values of the parameters Z_n and C_n . The value of L is then determined by applying (2) to the center frequency; knowing L , the product $Z_{01}C$ in (4) is fixed from the chosen value of C_n . The value of C is generally determined by the bounds of the design problem such as the required gap distance or the capacity of the tube electrodes in case of oscillator cavities; hence Z_{01} gets defined. The rest of the design requires only the determination of the diameters d_1 , d_2 , and D for the appropriate characteristic impedances keeping in mind that larger diameters give better Q_0 , while a possibility of circumferential modes limits the average circumference to less than the lowest wavelength.

A cold test model of a cavity with a range of 1100 to 1900 mc was designed to test the principles outlined above. The curves of $Z_n=3$ were chosen due to their reasonable linearity consistent with good tuning range. The mechanical structure of the cavity is shown in Fig. 5. The two center conductors are supported with the requisite spacing by being clamped to an outside frame which forms the base of the whole structure. The outer cylinder is mounted concentric to these conductors and it slides over the center conductor assembly. Accurate linear motion is imparted to the outer cylinder by means of a micrometer head having threads with one millimeter pitch; there are two hundred circumferential divisions, and motion adjustability of nearly 10^{-4} cm is thereby derived. An inherent backlash of about 0.005 cm exists; hence care is taken to make all adjustments in one direction only. The important dimensions of the cavity are $L=4.967$ cm, $D=4.0$ cm, $d_1=3.0$ cm, $d_2=1.75$ cm, and t is adjustable. The zero position on the micrometer scale corresponds to the case when the inner conductor d_1 is flush with the left wall of the cavity.

The feeding-in of the RF signal is in a completely symmetric manner. A tiny probe protrudes through the center of one of the inner conductors at the capacitive gap and delivers the RF signal to the cavity from an ordinary flexible coaxial cable which is brought in along the middle of the tube forming the center conductor d_1 .

B. Frequency Measurements

Measurements were first made on the cavity before plating and installation of spring fingers in order to assure that the cavity configuration was as close as possible to the theoretical design. As will be shown later, these changes lead to a perturbation of the frequency. For this experiment, the bearing surfaces were made to the best possible sliding fit and properly aligned in all

respects to ensure a good contact. A standard method⁵ was used for obtaining the curve of resonant frequency vs cavity scale reading for two gap distances [0.42 cm which corresponds to approximately $1\mu\mu f(C_n=0.1)$, and 0.21 cm which gives twice as much capacity ($C_n=0.2$)].

Fig. 6 shows the measurements (curves B) as well as the calculations (curves A) of tuning characteristics for these two gap spacings; it is noted that the measured curves exhibit an appreciably linear behavior, perhaps slightly better than the theoretical curves. For comparison, a tuning curve (curve D shown dotted) is also computed for the usual type of singly re-entrant cavity (*i.e.* the capacitance terminated coaxial line) in the same general range; the improvement in linearity by back-to-back tuning becomes quite apparent. By fitting the best

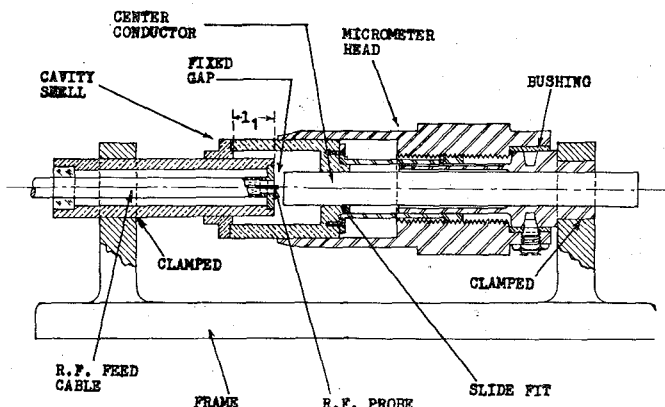


Fig. 5—The experimental resonator.

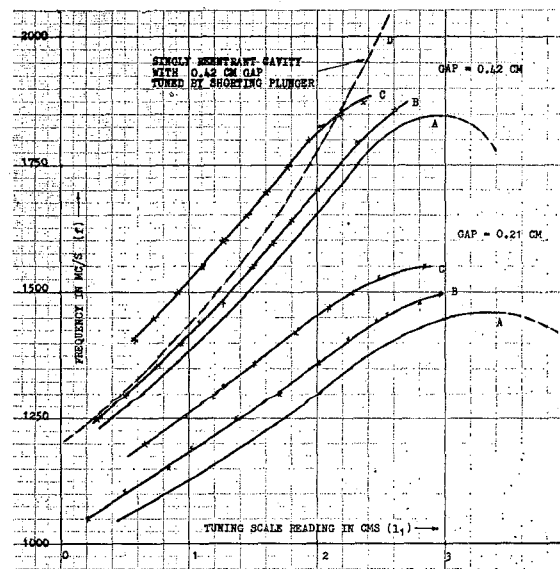


Fig. 6—Comparison of measured and calculated readings for gap distances of 0.42 cm ($C_n=0.1$) and 0.21 cm ($C_n=0.2$). A gives calculated values; B gives measured values without spring fingers; C gives measured values with spring fingers and silver plating.

⁵ E. L. Ginzton, "Microwave Measurements," McGraw-Hill Book Co., New York, N. Y., pp. 413-417; 1957.

straight line through our measured values, it can be checked that departure from linearity is much less than 1 per cent for the whole range. For the larger capacitance value, the linearity appears to be further improved, although the tuning range is much reduced.

It is noticed that the measured curves have shifted upwards and leftwards from the calculated curves for both values of gap distance. An inquiry into the possible reasons for this difference between theory and experiment yields a better insight into short-comings of the first order theory.

- 1) A small systematic error is introduced due to the finite thickness of the capacitive gap. In the experiment, the micrometer scale is referenced from the left wall of the cavity and, in any given position, measures the distance from the wall to the end plate of the larger central conductor. Where the gap thickness is truly negligible this would not cause an error, but for appreciable gap width (0.42 cm and 0.21 cm in our experiment) the distance l_1 should be measured to the center line of the gap as the appropriate reference; hence all measured readings would be shifted to the right by half the gap width.
- 2) Consider the RF field configuration near the gap as sketched in Fig. 7. Our design did not take into account the effects of the "fringe" fields on the capacity at the gap but merely assumed a lumped capacitance of the ideal parallel-plate-type calculated from the average area of the end surfaces of the two center conductors. In practice, the "effective" capacitance under RF operation is different and is determined by the field lines exchanged between the two center conductors. Hence the lines terminating on the outer cylinder indicate a reduced effective capacitance. Resonance would therefore be indicated at a slightly higher frequency.
- 3) Due to the same fringing effect, the effective lengths of the coaxial lines have changed. This is shown by the distance marked A on Fig. 7 which is the distance from the gap center to the surface of revolution which separates the fields of the left-hand coax from the fields of the righthand coax. It is easily seen that the direction of the error is such as to explain the differences between theory and experiment.

A little thought will show that the errors due to 2) and 3) will be larger for larger values of Z_n and for narrower gaps, since the differences in diameters of the two central conductors, as will a narrower gap, will cause the actual capacitance value to differ considerably from that calculated on the average area basis.

In preparation for a proper measurement of Q_0 , spring-fingers were subsequently installed at the sliding

contacts and the RF surfaces were plated with a coat of about 20 microns of silver. Frequency measurements were repeated in order to assess the change caused by these additions; these measured curves are also shown in Fig. 6 (marked C). It is clear that these changes have caused a perturbation of nearly 100 mc in the frequency due to the reduction in volume and the consequent change in the resonant structure; however, linearity is not at all impaired.

C. Measurement of Q

The first order formula for calculating the Q_0 of this cavity was derived in Section III. When applied to the present design, a curve of Q_0 vs the tuning position can be calculated; such a curve is shown in Fig. 8. It is of interest to note the general trend of the curve which indicates a similarity in general form to the slope of the tuning curve. We see that Q_0 is reasonably high in the region of interest to us (namely the linear tuning region on the left hand side) and that it shows a slight rise with frequency; the rapid fall in the region beyond the linear range is of little consequence since the cavity is not intended for use in that region.

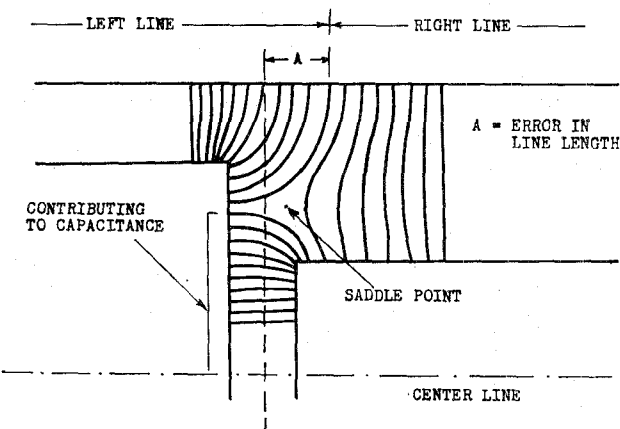


Fig. 7—Probable configuration of electric field lines near the gap.

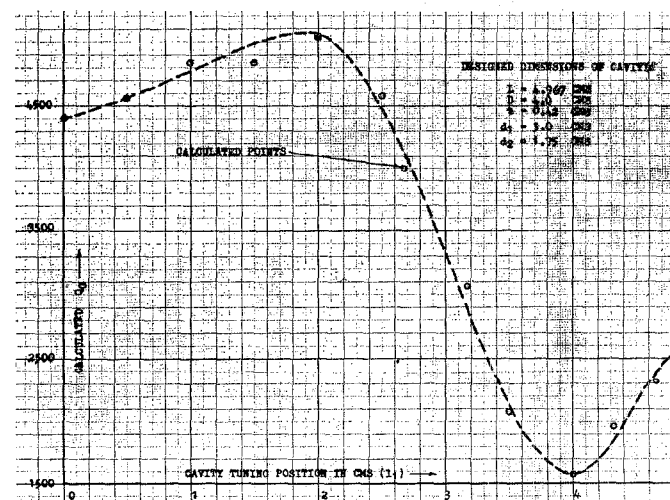


Fig. 8—Calculated Q_0 of the resonant system.

Practical measurements of unloaded Q_0 for a gap distance of 0.42 cm were carried out using the impedance method,⁵ and are shown in Table I together with the corresponding calculated values.

TABLE I

COMPARISON OF CALCULATED AND MEASURED VALUES OF Q_0

Measured frequency in megacycles per second	Tuning position in centimeters	Measured Q_0	Corresponding theoretical Q_0
1500	0.85	1125	4700
1600	1.55	1280	4950
1800	1.8	1720	5100
1870	2.50	900	4400
1690	3.49	575	2100

As can be expected, the measured values of the unloaded Q_0 are about 25 per cent of the theoretical values. This difference is a usual one in case of Q_0 measurements and is due to losses which are not accountable by the simple theory. Losses at the shorting end, imperfect spring contacts, unpolished surfaces, dirt, scratches, capacitance losses at the gap, no losses etc., account for this difference.

V. CONCLUSION

The first-order theory of back-to-back tuning has been derived and shown to agree reasonably well with the experimental results. Both theory and experiment

show that the resonator tuning characteristic obtainable by this method is linear for all practical purposes over a large frequency range. By appropriate design, various frequency ranges and tuning slopes can be obtained. The theoretically expected values of unloaded Q_0 are in the vicinity of 4500, while in actual practice values around 1200 are obtained in the useful range of linear tuning.

The method is, in general, applicable to any form of resonant system where quarter-wave line sections can be employed. For instance, for frequencies in the VHF range, the method can be applied with Lecher lines; in the UHF range, coaxial-type lines are more convenient. The presence of a capacitive gap makes the system especially adaptable where interaction with an electron beam is intended. Due to the simple construction, convenient size, nonharmonic modes, and good mode separation, this method should hold promise of valuable application over a wide frequency spectrum.

VI. ACKNOWLEDGMENT

The authors gratefully acknowledge the valuable help of Dr. H. D. Doolittle of Machlett Laboratories, Inc., Springdale, Conn., for initiating the idea and giving a start to the investigation; and also the assistance of B. Rama Krishna Rao and Ravindra Babu (both of this Institute) in making the many measurements and plots.

Equivalent Circuits for Small Symmetrical Longitudinal Apertures and Obstacles*

ARTHUR A. OLINER†

Summary—Formulas based on small aperture and small obstacle theory are presented for the determination of equivalent circuits for symmetrical longitudinal apertures and obstacles. These formulas are then applied to several examples of practical interest, including aperture discontinuities in trough waveguide and an obstacle array of interest to anisotropic radomes.

I. INTRODUCTION

THE evaluation of equivalent circuits for waveguide discontinuities often involves the solution of a boundary value problem of considerable complexity. For the class of so-called "small" apertures and obstacles, however, this evaluation becomes particu-

larly simple when the problem is properly phrased. A small aperture or obstacle is one which is located far from the guide walls and whose dimensions are small compared to a wavelength. Under these conditions, the distortion of the field lines in the vicinity of such a small aperture or obstacle, due to some specified excitation, is essentially independent of the cross-sectional shape of the containing waveguide, and depends only on the nature of the excitation and the physical shape of the aperture or obstacle. The quantity which characterizes the aperture or obstacle and which is a function only of its physical geometry and the type of incident excitation is the *polarizability*; since the aperture or obstacle is small compared to wavelength, the polarizability may be determined under static conditions. The function of small aperture or obstacle theory is then to relate the polarizability to the location of the aperture or obstacle within the containing waveguide and to the appropriate

* Manuscript received by the PGMTT, August 28, 1959. The major portion of this work was performed at the Microwave Research Institute of the Polytechnic Institute of Brooklyn under Contract No. AF-19(604)-2031, sponsored by the Air Force Cambridge Research Center.

† Microwave Research Institute, Polytechnic Institute of Brooklyn, Brooklyn, N. Y.